



## COB-2021-1250

### DETERMINING SPECIFIC CUTTING ENERGY BY SPINDLE POWER WHEN MICRO-MILLING Ti-6Al-4V

#### Rodrigo Ferreira

Federal Institute of Pernambuco, Department of Control and Industrial Processes, Av. Luís Freire, 500 - Cidade Universitária, CEP 50740-545, Recife – PE

São Carlos School of Engineering, Department of Mechanical Engineering, Av. São Carlense, 400, CEP 13566-590, São Carlos – SP

rodrigoferreira@recife.ifpe.edu.br

#### Ricardo Arai

Federal Institute of São Paulo, Department of Aviation Maintenance Technology, Estrada Municipal Paulo Eduardo de Almeida Prado, CEP: 13565-820, São Carlos - SP.

ricardo.arai@gmail.com

#### Alessandro Roger Rodrigues

São Carlos School of Engineering, Department of Mechanical Engineering, Av. São Carlense, 400, CEP 13566-590, São Carlos – SP

roger@sc.usp.br

#### Reginaldo Teixeira Coelho

São Carlos School of Engineering, Department of Production Engineering, Av. São Carlense, 400, CEP 13566-590, São Carlos - SP.  
rtcoelho@sc.usp.br

**Abstract.** *Micro-milling is a promising process to create microtextures on Ti-6Al-4V alloy surfaces for implants; however, tool wear is a problem. High-resolution cameras and acoustic emission sensors are some technologies used for checking wear. Most equipment used for micro-milling has a spindle with high-speed electric motors, and the acquisition of power can be an alternative to monitor the process and assist the existing techniques. This study proposes a technique for applying the Savitzky-Golay filter (SGf) to process cutting power signal when milling Ti-6Al-4V micro-slots to obtain the specific cutting energy (SCE) and monitor the power. The experiments were conducted using a high-speed electric motor, acquiring power signals during cutting. The Origin software with a smooth filter package was used to process the cutting power data. SCE values for feeds per tooth of 3, 6, 12, and 15  $\mu\text{m}$  were calculated using the proposed method and compared with the primary literature. Treatment of the power signal through SGf was appropriate and enabled the use of cutting power to obtain the SCE as a function of  $f_z$ . This method can be an alternative to evaluate SCE during micro-milling.*

**Keywords:** *Micro-milling, Specific cutting energy, Ti-6Al-4V, Savitzky-Golay filter.*

## 1. INTRODUCTION

Micro-milling is a well-researched material removal fabrication process applied in the meso- and micro-scales to electronic components, microfluidic devices, micro-molds, and the medical field (Chen et al., 2021). Despite this range of applications, there are critical challenges to be overcome, such as elucidating wear mechanisms for specific classes of materials (Colpani et al., 2019), selection of coatings (Ziberov et al., 2020), process monitoring through the use of specific sensors, and choice of grain size for suitable applications (Rodrigues and Jasinevicius, 2016). Titanium alloys, more specifically the Ti-6Al-4V alloy, is one of the alloys with the largest number of contributions to the study of micro-milling because it is an aeronautical and biomedical alloy. However, this alloy faces real challenges, such as low thermal conductivity and high specific heat, resulting in low diffusivity and hindering dry cutting. Regarding its mechanical properties, Ti-6Al-4V presents high yield stress and strength limit values, associated with hardness of 30-36 HRc (ASTM F136) and microstructure formed by alpha and beta phases, which hampers its cutting. Forming the built-up edge (BUE) becomes a real challenge to the quality of the micro-milled surface. Therefore, monitoring systems are essential to indicate any change in the state of the micro mill, to assess whether it is time to change the tool or even to stop the process and assess the surface state. However, all these difficulties occur on small scales, which hinders the visualization of their aspect. These micro-scale machining process monitoring systems include acoustic emission sensors (Malekian et al., 2009), dynamometric platforms, and high-resolution cameras (Malekian et al., 2009).

Some articles have proposed the fusion of sensors to monitor the process, but the high cost of some sensors is usually a great barrier, e.g., piezoelectric dynamometers (Cao and Li, 2015). In reality, dynamometers are usually not used at shop floor level for large-scale production of micro-components. Thus, some studies have recommended the use of cheaper sensors that are less invasive in the manufacturing process, and thus more appropriate to industrial applications. Other papers have suggested that the cutting processes be monitored directly from CNC or spindle motor through electrical current and voltage, but the results differ from those of dynamometers if the collected raw data are not properly treated by statistics (drifts, filters, transforms, artificial intelligence, artificial neural networks, etc.) or calibrated due to thermo-electric-mechanical losses (motors, bearings, guides, etc.).

In this sense, Oliveira et al. (2021) proposed to apply acoustic emission to investigate the signal difference under dry cutting and minimum quantity of lubricant (MQL) in the micro-milling of slots in the Inconel 718 alloy. Ribeiro et al. (2020) demonstrated that the acoustic emission technique could assess cutting stability and compare workpiece materials with different grain sizes when subjected to the same cutting conditions. Varghese et al. (2020) proposed to investigate the end of life of micro end mills using force signal analysis and images of micro end mills using the machine learning technique, and demonstrated that force signal analysis is more suitable than image investigation.

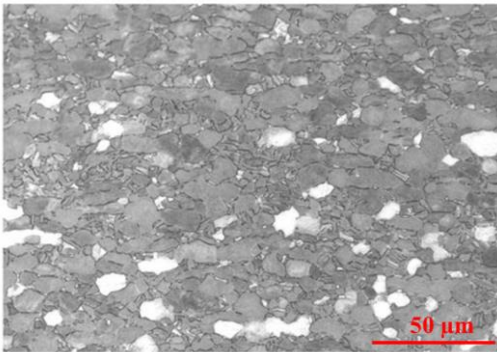
Rezaei et al. (2018) showed that the specific cutting energy (SCE) obtained through mini-dynamometers in micro-milled Ti-6Al-4V slots varied according to the type of cooling (dry and MQL) and cutting speed ( $v_c$ ) used. Thus, they were able to determine the minimum chip thickness value according to cooling and  $v_c$ . Wang et al. (2017) demonstrated that is possible to correlate the electric current coming from the high-speed motor of the spindle with micro-mill wear. Zhang et al. (2020) proposed a mathematical model to calculate the cutting power through material data and cutting forces measured by dynamometry in micro-milling. However, even using a dynamometer, those authors obtained higher cutting power than that expected for the adopted parameters.

In this context, this paper proposes a calibrated mathematical method to obtain the SCE in micro-milling through the spindle speed controller, since SCE is one of the most important parameters used in micro-scale cutting. To this end, Ti-6Al-4V alloy was micro-milled by varying feed per tooth and the SCE values obtained were validated by the specific literature.

## 2. EXPERIMENTAL PROCEDURE

Ti-6Al-4V alloy material used for micro-milling was provided by Engimplan and processed by lamination and annealing (thermomechanical history by the US-based company Timet. The microstructure and material properties data are organized in Table 1. The grain size ( $GS \sim 10 \mu\text{m}$ ) was obtained using the ASTM E112-12 standard by applying the intercept method.

Table 1 - Material specifications, microstructure, and mechanical/physical properties

Material	Microstructure	Properties
Ti-6Al-4V phases: $\alpha + \beta$	500X Transverse	Hardness = 305 HV
		$E = 114 \text{ GPa}$
		$\sigma_e = 810 \text{ MPa},$ $\sigma_{LR} = 900 \text{ MPa}$
		$\varepsilon = 18\%$
		$GS \sim 10 \mu\text{m}$

In this research, micro-milling is used for grooving using micro end mills in a vertical machining center with feed movement in the X direction in the XY plane of the machine table. The entire test was conducted without the use of a lubricating fluid. A Hermle C800U machine with a positioning accuracy of  $0.5 \mu\text{m}$  was used associated with a high-speed motor (HES 501, Nakanishi) with a maximum speed of 50,000 1/min.

Cutting speed ( $v_c$ ) and axial depth of cut ( $a_p$ ) were maintained constant in all four tests performed, using the values of 44 m/min and  $50 \mu\text{m}$ , respectively, varying the feed per tooth ( $f_z$ ). The  $f_z$  used were 3, 6, 12 and  $15 \mu\text{m}/\text{tooth}$ . The radial depth of cut was the diameter of the cutter used in the tests,  $a_e = 500 \mu\text{m}$  (full cut). Mitsubishi solid carbide end mills (model MS2MS D0050 N015) with a nominal diameter of  $500 \mu\text{m}$ , two cutting edges, cutting length of 1.5 mm, and TiAlN coating were used. For each new test configuration ( $f_z$ ), a new tool was employed. All tests were repeated once and, for each repetition, a new tool for the  $f_z$  condition was used. All tools were checked before testing by using a confocal

microscope so that they were used without compromising the major and minor cutting edges, and with no other wedge damage on the clearance and rake surfaces.

The experimental setup is illustrated in Fig. 1, showing the characterization of the tool by SEM (Fig. 1a), the positioning of the sample on the machine table, and the acquisition system used to obtain and visualize the power signal (Fig. 2b). Workpiece blocks of size 13 x 10 x 10 mm were prepared for micro-milling according to Fig. 1c.

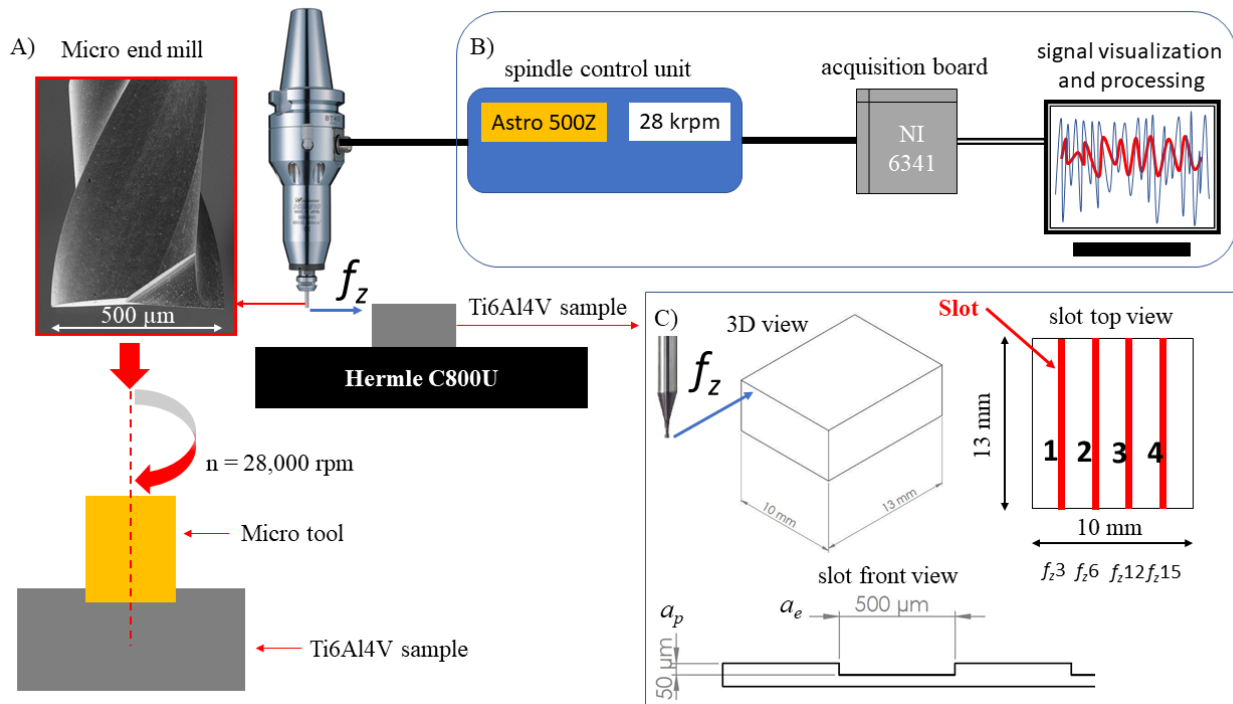


Figure 1 - Experimental setup: A) micro end mill; B) acquisition system; C) slot geometry.

## 2.1 Methodology for analyzing the acquired power data

Monitoring of the power and spindle rotation signals was performed from the connection between the pins referring to the CN2 output of the NSK Astro-E500 controller to BNC cables made for communication with the National Instruments NI USB-6341 acquisition board.

In the program developed in the LabVIEW platform, the Virtual Instrument (VI) receives data from an acquisition board dedicated to the power and rotation signals, collecting the signal at a rate of 5 kHz. Using the NSK catalog, the maximum power delivered and voltage for the signal output (CN2 - pins 12 and 13) of the controller are 250 W and 15 V, respectively. Thus, the calibration values for the power signal are 16.667 W/V. The generated files have an “lvm” extension and are composed of time, power and rotation values.

Power signal processing was performed in the Origin Lab 2018 software. This software contains a variety of filters and allows fast processing. The analysis and processing of the power signal are a very interesting challenge due to the behavior of this power signal and the number of maximum and minimum points that occurs during micro-milling (Figure 2). SCE calculation can be strongly influenced, depending on the processing technique utilized. Thus, the method proposed by this paper is compared with those found in the literature, which are presented in the Results and discussion section.

Figure 2 shows five test machining intervals: no contact (1); gradual tool immersion into workpiece (2); full cutting (3); gradual tool exit from workpiece (4); no contact (5). The minimum and maximum feed rates are 168 and 840 mm/min, and thus the signal processing windows are 4.46 and 0.89 s for the smallest and highest feeds per tooth, respectively, for a cutting distance of 12.5 mm (interval 3). A tool displacement of 12.5 mm guarantees that tool diameter half is engaged in the workpiece entry and exit.

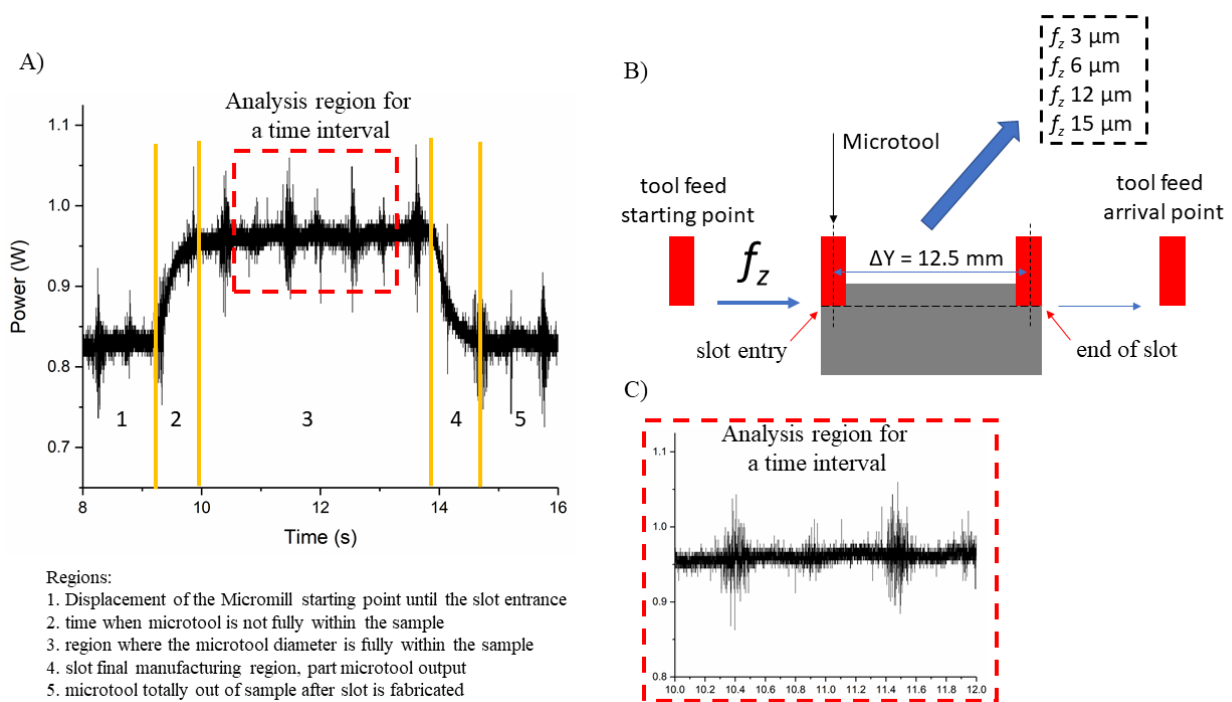
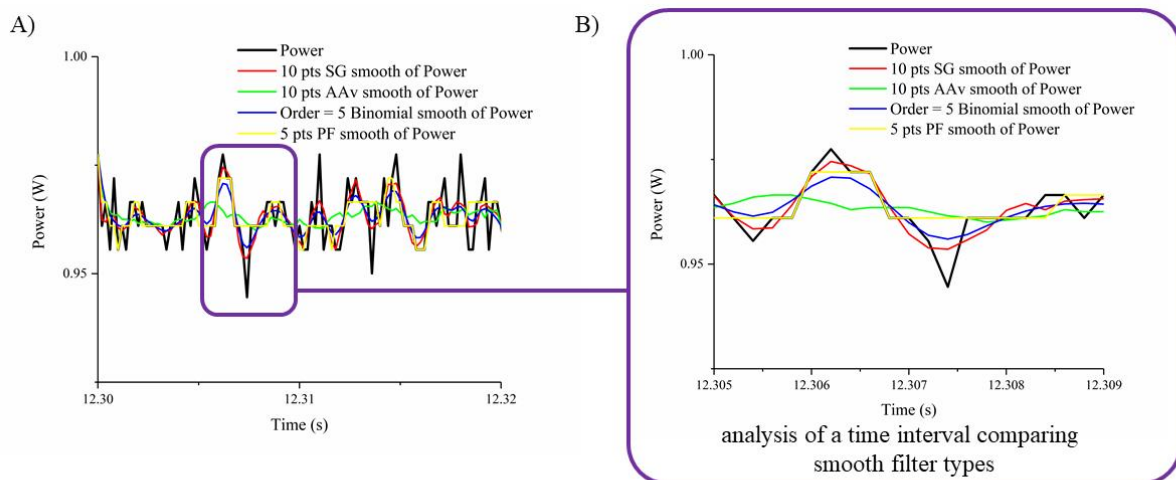


Figure 2 - Power graph obtained during micro-milling.

The Savitzky-Golay filter (SGf), which is one of the types of filters of the Smooth class, was applied to power signals. The SGf performs a local polynomial regression around each point and creates a new smoothed value for each data point. This method is superior to the moving average calculation because it tends to preserve data characteristics, such as peak height and width, which can be “cut-off” by the moving average. To increase the smoothness of the curve, the window size or the number of points used can be increased; these regression degrees vary from 1 to 5.

The decision criterion for using the SGf was compared with other Smooth filters, such as the Moving Average - also known as Adjacent Averaging (AAv), Percentile Filter, and Binomial. However, the most suitable in some tests (Figure 3a) was the SGf, which showed better preservation of the power signal characteristics as a function of time. This analysis took a power signal discretization for an interval of 20 ms (Fig 3a).

The filters analyze the signal's peaks and valleys, so the filter that best fits these original peaks and valleys can be the candidate of choice (Lavaud et al., 2019). For example, a 4 ms interval of the power signal detailed in Figure 3b shows that the smooth SGf is the most suitable for signal treatment.



Savitzky-Golay (SG); Adjacent Averaging (AAv); Binomial; Percentile Filter (PF)

Figure 3 - Analysis of smooth filters: A) analysis of the behavior of filters for an interval of 20 ms; B) window for a 4 ms interval detailing peaks and original values and a comparison between filters.

Tests for filter window employed between 150 and 2,500 points, and polynomial fitting of degree 5. After using the SGf, the area below the curve indicated by the red line (Fig. 4) was calculated. The value numerically represents the energy consumption for slot machining (0.05 x 0.5 x 12.5) mm<sup>3</sup>.

SCE calculation needs the energy used during a period of time, and can be obtained through the integral of the power after the signal processing as a function of time, according to Eq. 1. The volume removed from the workpiece material in a period of time can be calculated using of the following variables: micro tool diameter, depth of cut, and feed rate at a time interval ( $\Delta t$ ), as in Eq. 2. After obtaining the energy used in cutting and the volume removed from the material, the  $SCE_{Power}$  is obtained through Eq. 3.

$$E(t) = \int_{t_1}^{t_2} P dt \quad (1)$$

$$V(t) = \frac{(doc \ \phi_{tool}) (f_z \ z n \Delta t)}{60} \quad (2)$$

$$SCE_{Power} = \frac{E}{V} = \frac{J}{mm^3} \cong GPa \quad (3)$$

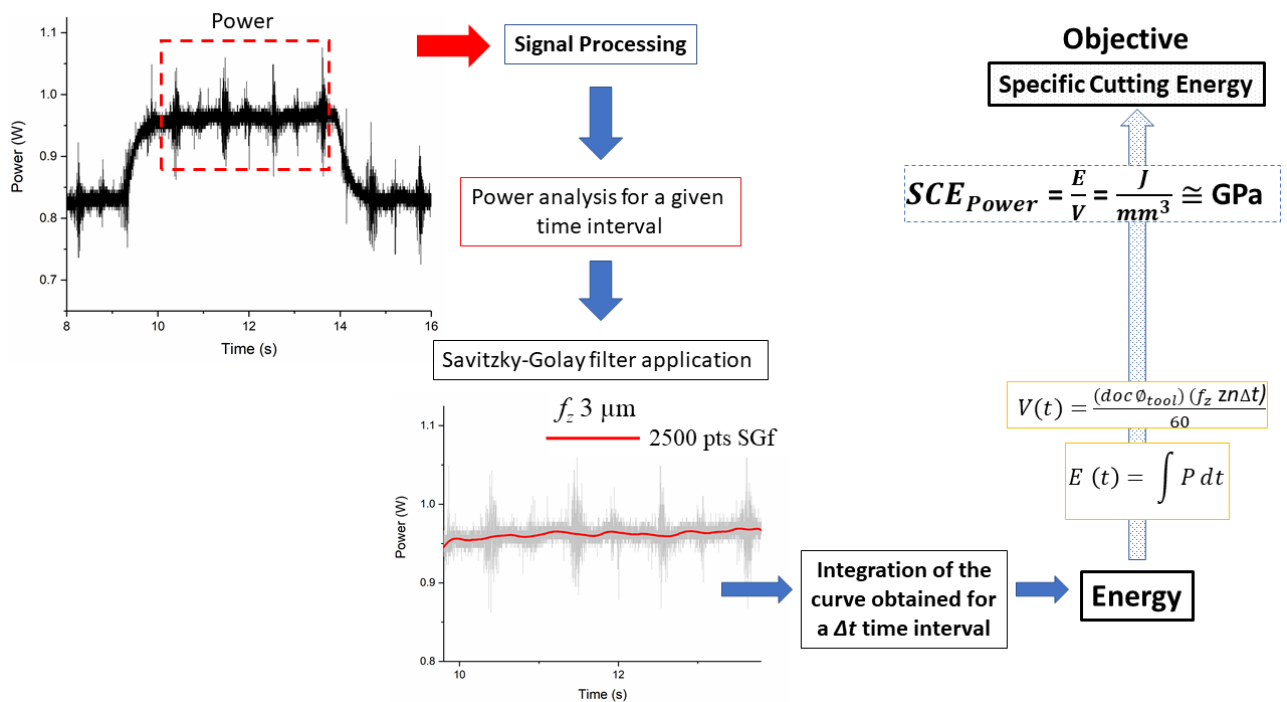


Figure 4 - Signal processing diagram using the Savitzky-Golay filter for the power signal.

### 3. RESULTS AND DISCUSSION

Figure 5 shows the graphs of the acquired powers during slot micro-milling. The graph in Fig. 5a shows the most extended time interval for power curve integration. This longer time interval is due to the smaller feed per tooth. This larger window allows the calculation of energy in several time intervals, and at low feeds it can facilitate monitoring the tool wear. For feeds per tooth of 12 and 15  $\mu m$ , the power graphs have similar curves and show sloped regions related to the full cutting. In cases where the feed rates are larger, it is suggested that the workpieces be milled longer in order to reach as close as possible the power signal steady state. The power signal behavior for 6  $\mu m$ /tooth seems to be a transition between constant and growing power.

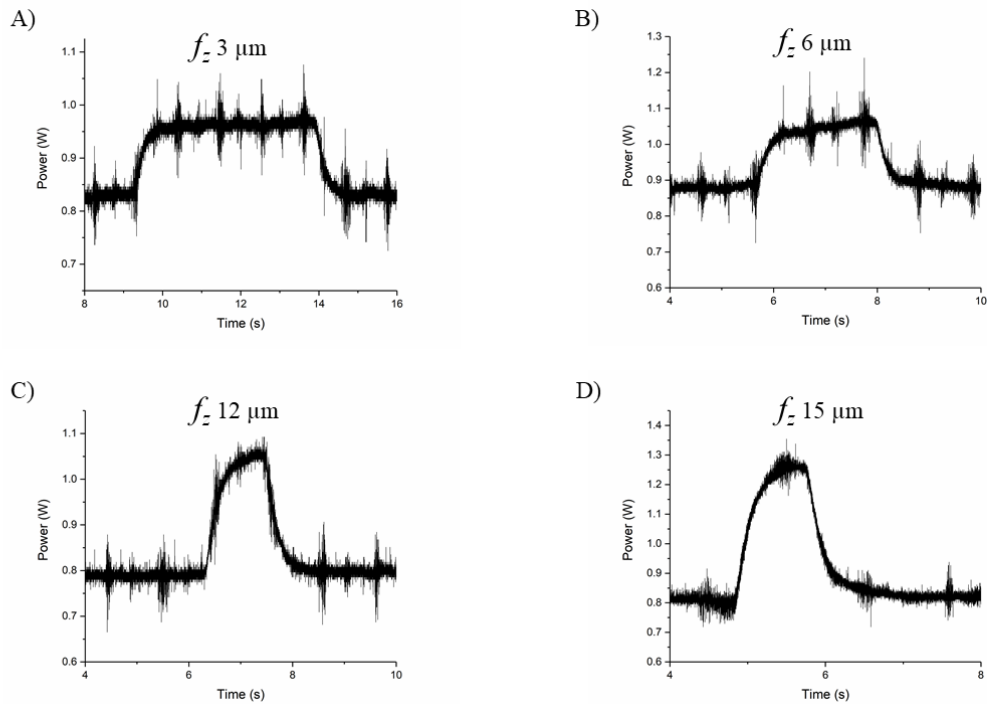


Figure 5 - Power graphs obtained for each value of feed per tooth.

Figure 6 shows the graphs of the regions where the micro tools engagement is total. It is possible to observe a decrease in the number of points used for the curve interaction obtained through the SGf (Fig. 6a and 6d). This decrease is due to the reduction of the analysis window for larger feeds; however, it is worth noting that, even with difficulty in optimizing the number of points, it is possible to see that the application of this smooth filter type assists in visualizing the greater curve slope resulting from the larger feed. This effect is a common feature of DC electric motors, and is correlated with increased torque due to increased cutting force as a function of feed (Altintas, 1992). It is essential to report that the cutting thickness varies along the edge movement during micro-milling. When the maximum thickness is reached, the motor electric current increases to compensate the greater tool resistance to workpiece material removal (higher cutting force).

Wang et al. (2017) also reported the effect of this slope on the monitored electrical current signal with the micro-milling time, and this fact corroborates our results, since electrical power is associated with voltage and current, both in phase.

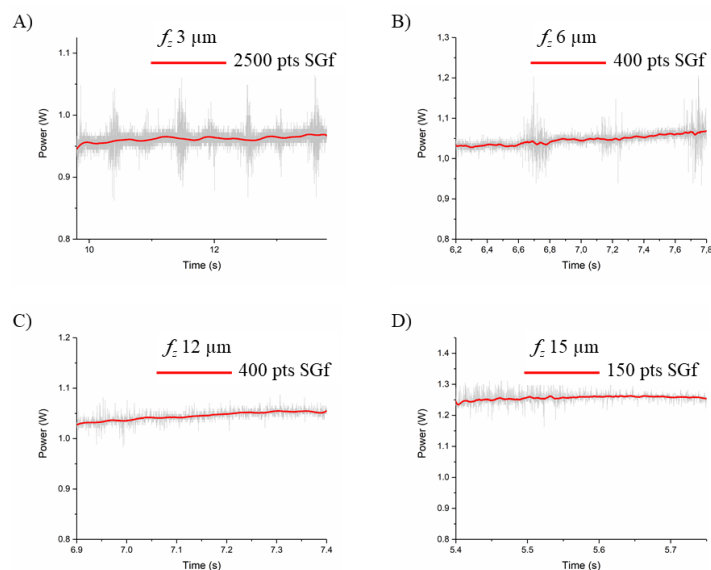


Figure 6 - Graphs after applying the Savitzky-Golay filter.

The energy calculated from each graph (Fig. 7) allowed us to obtain the SCE for the proposed tool feed rates (Fig. 7b). For comparison, Fig. 7a shows the SCE obtained by Campos et al. (2020) through a dynamometric platform when varying tool feed between 0.5 and 4  $\mu\text{m}/\text{tooth}$ . In this study, we extrapolated the results measured by Campos et al. (2020) by considering the same experimental tool feed rates in order to compare the SCE curve that we obtained by means of the power signals. Figure 7b shows that the SCE values are very close to each other. The difference is more significant at smaller feed rates, but this difference tends to a minimum at large tool feeds. However, it should be noted that the SCE values were obtained using different techniques, as well as distinct cutting parameters. These differences affect the results.

Given the high cost of piezoelectric dynamometers, SCE data as a function of tool feed when milling the Ti-6Al-4V alloy at micro-scale are scarce. Equation (4) shows the relationship between  $SCE'$  and  $SCE_{dyn}$ , in which  $SCE'$  is the specific cutting energy calibrated by that obtained by dynamometry ( $SCE_{dyn}$ ) considering an R-function dependent on tool feed (Equation (5)) and the  $SCE_{Power}$  obtained through power. It is essential to note that, once calibrated, the method can be used under the same cutting conditions, and thus allows the use of power data to monitor the process. From the relations of  $R$  obtained as a function of each  $f_z$ , it is possible to obtain a linear trend line, as shown in Figure 7c.

$$SCE' = R \cdot SCE_{power} \quad (4)$$

$$R(f_z) = \frac{SCE_{dyn}(f_z)}{SCE_{Power}(f_z)} \quad (5)$$

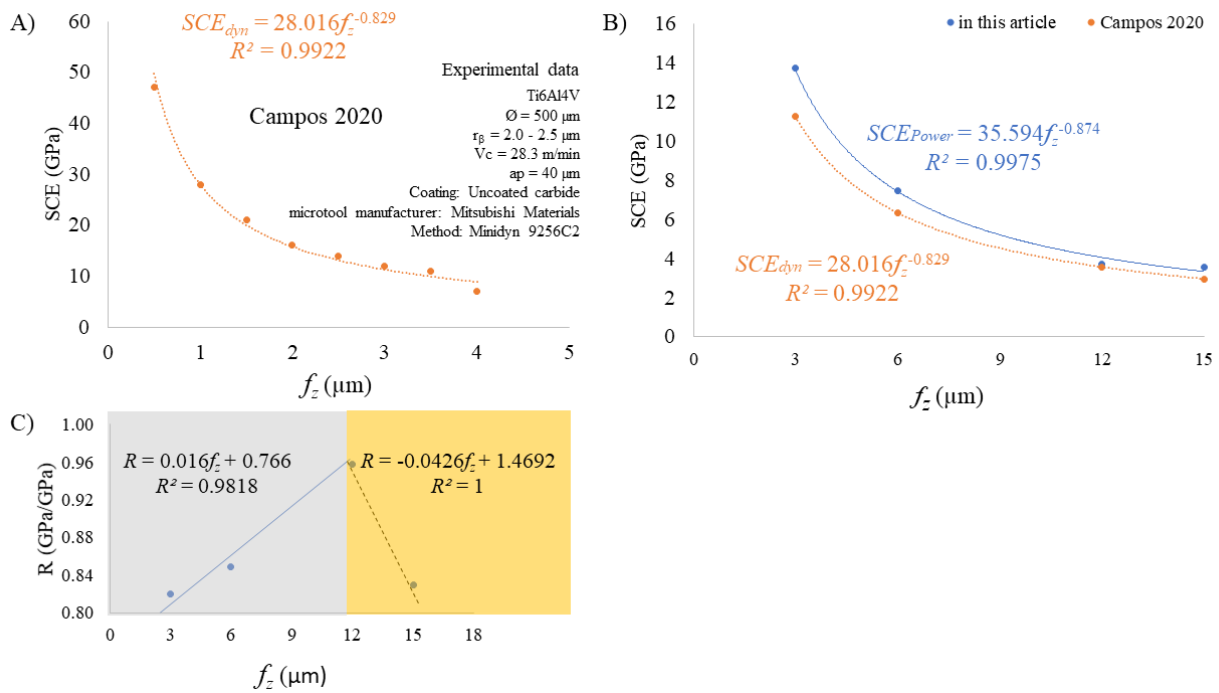


Figure 7 - SCE vs. tool feed and R-function of calibration: A) SCE by Campos et al. (2020); B) comparison between the current paper and Campos et al. (2020); C) R-function of correction  $SCE_{dyn}$ .

By means of the relations presented in Fig. 7c, Eq. (4) can be rewritten for two tool feed rate domains. For tool feeds between 3 and 12  $\mu\text{m}/\text{tooth}$  and 12 and 15  $\mu\text{m}/\text{tooth}$ , Eqs. (5) and (6) can be used, respectively.

$$SCE' = (0.016f_z + 0.766)35.594f_z^{-0.874} \quad (5)$$

$$SCE' = (-0.0426f_z + 1.4692)35.594f_z^{-0.874} \quad (6)$$

The variable of correction,  $R$ , demonstrates that it is possible to obtain a direct relationship between feed,  $SCE_{Power}$ , and  $SCE_{dyn}$ . Once corrected specific cutting energy is obtained, power measurements can be used to monitor the micro-milling process.

A gradual decrease in specific cutting energy when increasing feed per tooth is not a complete parameter; therefore, Figures 7a and 7b should be carefully observed because show the size effect. The SCE deals with the energy used to remove 1  $\text{mm}^3$  in chip volume, so the electric motor power signal can be an essential parameter for monitoring the energy

used to remove material in the slot. However, it should be noted that the increase in  $f_z$  minimizes the SCE (Figure 7). Nevertheless, high values of  $f_z$  affect the surface integrity. In addition, the feed per tooth ( $f_z$ ) increasing the cutting force contributes to the increase in roughness and vibration (Assis, 2013).

The proposed methodology can be used by manufacturers of high-speed electric motors for spindles for some rotations, materials, and feeds in the case of micro-milling applications.

#### 4. CONCLUSIONS

This paper investigated the possibility of using the spindle power obtained through an acquisition system to calculate specific cutting energy (SCE). The methodology proved to be effective, although data with a dynamometric platform are scarce. It was also possible to obtain a correlation for the removed chip volume as a function of micro-milling time, and this allows the use of the methodology for short-time intervals at high tool feed. Data from the literature allowed us to establish mathematical correlations that enable calibration of the SCE obtained through power and of the  $SCE_{dyn}$  calculated by employing dynamometers. Growing power with cutting time for higher tool feed rates needs to be more comprehensively investigated. For these cases, longer slots are recommended for more reliable power measurements.

#### 5. ACKNOWLEDGMENTS

The authors thank Mitsubishi Brasil for providing the micro mills, Nakanishi for some technical clarifications, and FAPESP for funding the Hermle C800U machining center (grant no. 2016/11309-0). We are especially grateful to MSc. Kandice Ribeiro for developing the power data acquisition system on the LabVIEW platform.

#### 6. REFERENCES

- Altintas, Y., 1992. Prediction of Cutting Forces in Five-Axis Milling Using Feed Drive Current Measurements. *IEEE/ASME Trans. Mechatronics* 23, pp. 833–844. <https://doi.org/10.1109/TMECH.2018.2804859>
- Assis, C.L.F., 2013. Micro-milling of ultra-fine grain steels. Doctoral Dissertation, Graduate Program in Mechanical Engineering, University of São Paulo, São Carlos, Brazil. <https://doi.org/T.18.2013.tde-13082014-152804>
- ASTM F136 – 13: Standard Specification for Wrought Titanium-6Aluminum-4Vanadium ELI (Extra Low Interstitial) Alloy for Surgical Implant Applications. 2013. <https://doi.org/10.1520/F0136-13R21E01>
- Cao, Z., Li, H., 2015. Investigation of machining stability in micro milling considering the parameter uncertainty. *Adv. Mech. Eng.*, Vol 7, pp. 1–8. <https://doi.org/10.1177/1687814015575982>
- Chen, N., Li, H.N., Wu, J., Li, Z., Li, L., Liu, G., He, N., 2021. Advances in micro milling: From tool fabrication to process outcomes. *Int. J. Mach. Tools Manuf.*, Vol 160. <https://doi.org/10.1016/j.ijmachtools.2020.103670>
- Colpani, A., Fiorentino, A., Ceretti, E., Attanasio, A., 2019. Tool wear analysis in micromilling of titanium alloy. *Precis. Eng.* 57, 83–94. <https://doi.org/10.1016/j.precisioneng.2019.03.011>
- de Oliveira Campos, F., Araujo, A.C., Jardim Munhoz, A.L., Kapoor, S.G., 2020. The influence of additive manufacturing on the micromilling machinability of Ti6Al4V: A comparison of SLM and commercial workpieces. *J. Manuf. Process.*, Vol 60, pp. 299–307. <https://doi.org/10.1016/j.jmapro.2020.10.006>
- Lavaud, R., Rannou, E., Marie, J.F.S., Jean, F., 2019. Reconstructing physiological history from growth, a method to invert DEB models. *Journal of Sea Research*, Vol 143, pp 183–192. <https://doi.org/10.1016/j.seares.2018.07.007>
- Malekian, M., Park, S.S., Jun, M.B.G., 2009. Tool wear monitoring of micro-milling operations. *J. Mater. Process. Technol.*, Vol 209, pp. 4903–4914. <https://doi.org/10.1016/j.jmatprotec.2009.01.013>
- Oliveira, D., Gomes, M.C., Ziberov, M., Silva, M.B. Monitoramento do processo de microfresamento de inonel 718 através de sinais de acústica e vibrações. In *Proceedings of 11th Brazilian Congress on Manufacturing Engineering - COBEF 2021*. Brazil. <https://doi.org/10.26678/ABCM.COBEF2021.COB21-0013>
- Rezaei, H., Sadeghi, M.H., Budak, E., 2018. Determination of minimum uncut chip thickness under various machining conditions during micro-milling of Ti-6Al-4V. *Int. J. Adv. Manuf. Technol.*, Vol 95, pp. 1617–1634. <https://doi.org/10.1007/s00170-017-1329-3>
- Ribeiro, K.S.B., Venter, G.S., Rodrigues, A.R., 2020. Experimental correlation between acoustic emission and stability in micromilling of different grain-sized materials. *Int. J. Adv. Manuf. Technol.*, Vol 109, pp. 2173–2187. <https://doi.org/10.1007/s00170-020-05711-1>
- Rodrigues, A.R., Jasinevicius, R.G., 2016. Machining scale: Workpiece grain size and surface integrity in micro end milling. *Microfabrication and Precision Engineering: Research and Development*. Elsevier Ltd. <https://doi.org/10.1016/B978-0-85709-485-8.00002-4>
- Varghese, A., Kulkarni, V., Joshi, S.S., 2021. Tool life stage prediction in micro-milling from force signal analysis using machine learning methods. *J. Manuf. Sci. Eng. Trans. ASME*, Vol 143, pp. 1–7. <https://doi.org/10.1115/1.4048636>
- Wang, C., Huang, M., Chung, T.T., Young, H.T., Li, K.M., 2017. Tool condition monitoring with current signals for a low-power spindle. In *Proceedings of the 2017 IEEE International Conference on Applied System Innovation - IEEE-ICASI 2017*, pp. 686–689. <https://doi.org/10.1109/ICASI.2017.7988518>

- Zhang, X., Yu, T., Dai, Y., Qu, S., Zhao, J., 2020. Energy consumption considering tool wear and optimization of cutting parameters in micro milling process, *Int. J. Mech. Sci*, vol 178. <https://doi.org/10.1016/j.ijmecsci.2020.105628>
- Ziberov, M., de Oliveira, D., da Silva, M.B., Hung, W.N.P., 2020. Wear of TiAlN and DLC coated microtools in micromilling of Ti-6Al-4V alloy, *Journal of Manufacturing and Processes*, Vol 56, pp. 337–349. <https://doi.org/10.1016/j.jmapro.2020.04.082>

## **7. RESPONSIBILITY NOTICE**

The authors are the only responsible for the printed material included in this paper.